Microscopic Structure and Thermodynamic Properties of Bulk Copolymers and Surface-Active Polymers at Interfaces. 2. Results for Some Representative Chain Architectures

Doros N. Theodorou

Department of Chemical Engineering, University of California, Berkeley, California 94720, and Center for Advanced Materials, Lawrence Berkeley Laboratory, Berkeley, California 94720. *Received May 27, 1987; Revised Manuscript Received October 23, 1987*

ABSTRACT: A recently developed lattice model[1] is applied to probe the interfacial structure and properties of some representative polymers, consisting of two types of segments (A, B) with different affinities for the surface. The following cases are examined: (a) bulk systems of surface active molecules of the type AB_{r-1}; (b) triblock copolymers of the type $B_{r_B/2}A_{r_A}B_{r_B/2}$; (c) random copolymers of A and B; (d) a lipid bilayer membrane. In case a, preferential adsorption of A segments is found to lead to the development of perpendicular orientation of bonds with respect to the surface and to a narrowing of chain shapes in directions parallel to the surface. The dependence of structural features, of interfacial tension, and of the spatial extent of the anisotropic region on chain length and on the nature of segment/surface interactions is explored. In case b we observe significant chain organization effects, which result in a nonlinear dependence of interfacial tension on chain composition. In case c interfacial structure is very similar to that of a pure homopolymer, and interfacial tension depends linearly on the relative proportion of the two types of segments in the chain. Model predictions for the surface tension of block and random copolymers of ethylene oxide and propylene oxide are in agreement with experiment, without any adjustable parameters. In case d the orientation of bonds with respect to the surface is explored, using an appropriate definition of the order parameter; model results are consistent with NMR measurements on bilayer membranes of potassium laurate.

Introduction

In a previous publication[1] we introduced a site lattice model for the quantitative description of the interfacial behavior of bulk polymers consisting of two types of segments (A, B) that can interact differently with the surface. In this paper we apply our lattice approach to study the interfacial behavior of some representative chain architectures in the bulk. Predictions on structure and interfacial tension are compared to available experimental evidence. Our discussion of obtained results falls into three sections.

In section 1 we apply our theoretical development to bulk systems of chains of the type AB_{r-1}, where the surface active "head" A has a tendency for preferential adsorption on the surface over B segments. As already pointed out,[2] such systems are useful as quantitative models of resin/filler interfaces in composite materials in the presence of coupling agents, such as silanes. The effects of varying the chain length and the relative affinity of segment types A and B for the surface are investigated. A pronounced buildup of bond orientation and a drastic decrease in interfacial energy relative to the bulk B_r homopolymer are observed as the tendency of type A segments to bond to the surface increases.

Section 2 is devoted to a study of bulk copolymer/air interfaces. Triblock copolymers of the type $B_{r_B/2}A_{r_A}B_{r_B/2}$, as well as random copolymers consisting of A and B type segments in various proportions, are examined by using our lattice model. The chosen systems simulate specific poly(ethylene oxide)-poly(propylene oxide) copolymers, whose surface behavior has been studied experimentally. The interfacial structure of the triblock copolymer systems exhibits interesting features, due to the preferential adsorption of A_{r_A} blocks on the surface. The structure of random copolymers changes only little relative to the pure homopolymer case. Model predictions on the variation of interfacial tension with chain architecture and composition are consistent with experimental measurements.

In section 3 we show how our model can be used to explore the structure of a lamellar lipid bilayer membrane, consisting of short, surface-active molecules. This is a system studied by Dill and Flory[3] using a simple, bond lattice model approach, whose mathematical structure has been explored in ref 2. We compare our theoretical predictions to theirs, as well as to experimental evidence on bond orientation, obtained through NMR measurements.

The lattice model used in this work involves several simplifying assumptions; most drastic among those is the assumption of constant segmental density in the polymer phase up to the surface. Nevertheless, it is quite successful in predicting experimentally observed trends in both microscopic structure and macroscopic thermodynamic properties, based on information about the chemical constitution of polymer chains. Refinements can be introduced straightforwardly. Thus, the approach outlined here shows considerable promise as a first step toward the development of rigorous predictive methods for interfacial systems involving bulk polymers.

1. Interfacial Behavior of Bulk Systems of Macromolecules with a Surface-Active Head

As a first application of the site model of ref 1 we consider bulk systems, consisting of linear macromolecules of the general structure AB_{r-1}. Type A segments are assumed to have a greater affinity for the surface than type B segments; in the terminology of the model the surface interaction parameter $\chi_s > 0$. To keep our parameter space manageable, and also to ensure that assumption V (ref 1) is satisfied, we used a Flory interaction parameter of $\chi = 0$ in all systems examined. Structural and thermodynamic parameters were explored as a function of chain length (r) and relative tendency for adsorption at the surface (χ_s).

The model interfaces examined here are relevant to a variety of technically important materials. In composite applications segment A may be a basic (e.g., amine or carbonyl bearing) unit, incorporated in the chains during synthesis of the polymeric matrix, to anchor them on an acidic (e.g., silica) filler surface; or it may be an acidic (e.g., chlorine bearing) unit, used to promote adhesion with a basic (e.g., calcium carbonate) filler. Such specific acid/base interactions have been found crucial to the mechanical performance of composite interfaces.[4] Matrix/filler bonding via coupling agents, such as silanes, is another situation in which our model can be used, to probe the local

0024-9297/88/2221-1422$01.50/0

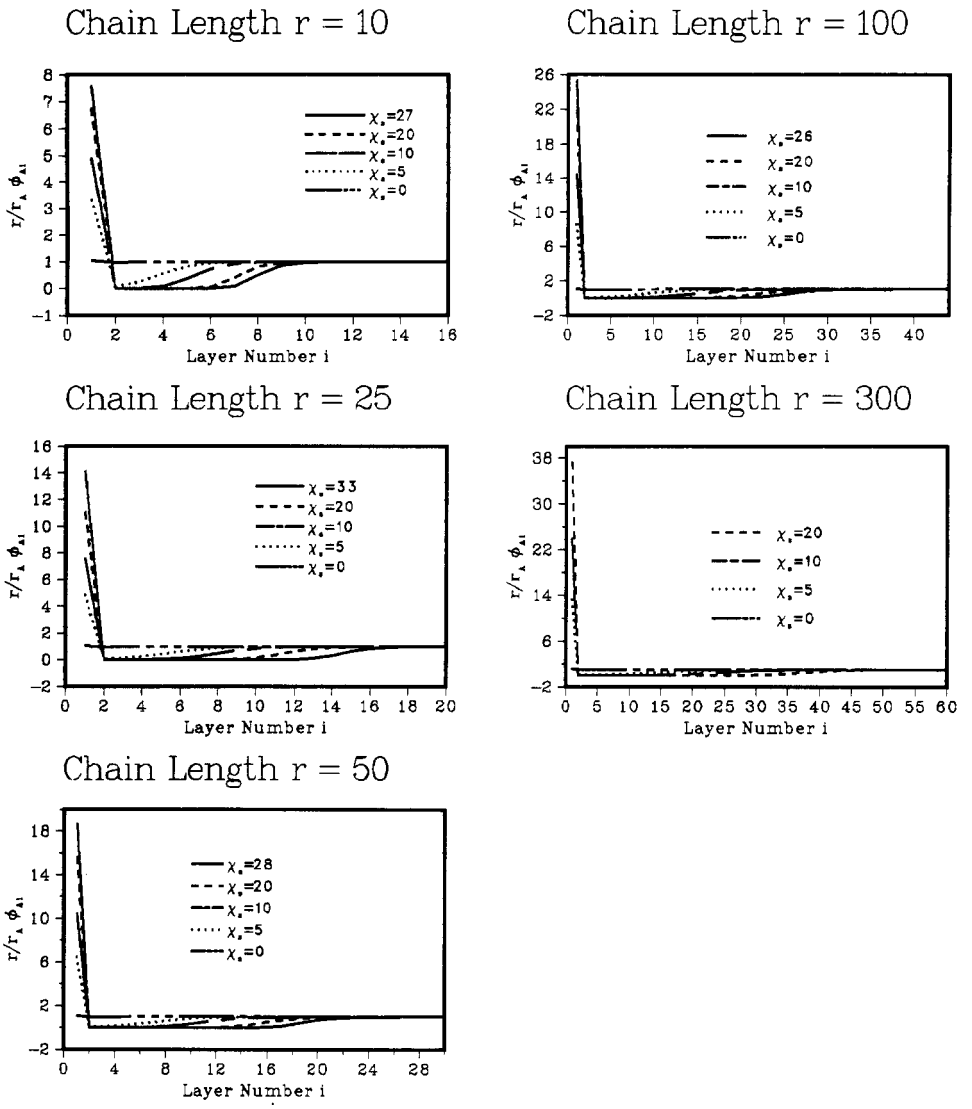

Figure 1. Spatial distribution of A segments for various values of the polymer–surface interaction parameter χ_s in bulk AB_{r-1} interfacial systems. Chain length: $r = 10$; $r = 25$; $r = 50$; $r = 100$; $r = 300$.

Table I
AB_{r-1} Interfacial Systems: Range of Parameters Studied

r	χ_s	m	r	χ_s	m
5	0–17	10	75	0–24	100
10	0–27	20	100	0–26	100
25	0–33	50	300	0–22	100
50	0–28	50	500	0–6	200

variation of mechanical properties as a function of distance from the interface (see discussion in ref 2). A third category of systems, in which our AB_{r-1} model offers a means of predicting interfacial structure and tension, is liquids consisting of long, surface-active molecules, such as aliphatic alcohols.

The range of parameters we employed in the studies reported here is summarized in Table I. For $\chi_s = 0$ the copolymer model reduces to that of a pure homopolymer, discussed in ref 5. Coincidence of the results obtained with those reported there was ascertained. Numerical computations for $\chi_s \geq 0$ were carried out as described in ref 1, Appendix B. A zeroth-order continuation scheme was used for runs with $\chi_s > 0$ at a given chain length. The number of layers m was in all cases sufficiently large for properties in the middle region, between the two interfaces, to be representative of the unconstrained bulk; interface structure and properties were found completely insensitive to further increases in m, for all cases listed in Table I. Thus, our model system is representative of a semiinfinite domain of surface-active polymer, adsorbed on a single flat surface.

Structural and thermodynamic characteristics of the studied AB_{r-1} systems are reported below.

A Segment Density Profiles. The spatial distribution of surface active A segments was computed for various (r, χ_s) combinations. The asymptotic value of the volume fraction ϕ_{Ai} at large distances from the interface is in all cases equal to

$$\lim_{i\to\infty} \varphi_{Ai} = \varphi_{A\infty} = \varphi^*_A = r_A/r \qquad (1)$$

This is in agreement with assumption V. In the case of AB_{r-1} chains examined here, $r_A = 1$. The reduced profiles $(r/r_A)\varphi_{Ai}$ are presented in Figure 1, to facilitate comparison among various chain lengths. In the pure homopolymer case ($\chi_s = 0$), a weak tendency for chain ends to concentrate on the surface layer is seen. The quantity $(r/r_A)\varphi_{A1}$ ranges from 1.0337 for $r = 10$ to 1.0897 for $r = 300$. This tendency is dramatically accentuated with increasing χ_s, as the surface active A-head adsorbs preferentially on the surface layer. Selective adsorption is accompanied by a depletion of the subsequent interfacial layers of A segments, as manifested by the sharp drop of φ_{Ai} between layers 1 and 2. This is because subsequent layers must necessarily accommodate the B segments belonging to the long tails of the adsorbed chains. The volume fraction φ_{Ai} rises gradually to its asymptotic unconstrained bulk value

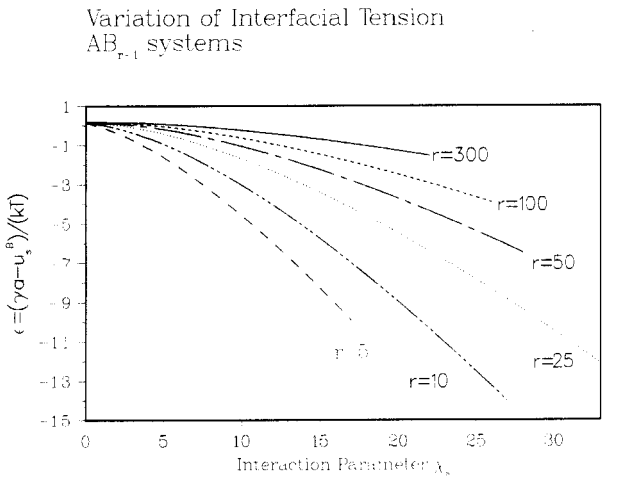

Figure 2. Variation of the nondimensionalized interfacial free energy relative to pure B monomer, $\epsilon = (\gamma a - u_s^B)/kT$, with the polymer surface interaction parameter χ_s in bulk AB_{r-1} polymer systems for various chain lengths r.

over a characteristic distance, which is an increasing function of χ_s and r. With increasing chain length the average volume fraction of A segments in the polymer decreases; nevertheless, the tendency of A segments to adsorb on the surface, as measured by the reduced quantity $(r/r_A)\varphi_{A1}$, becomes more and more pronounced. As an example, for $\chi_s = 20$ this quantity rises from 6.774 at $r = 10$ to 37.309 at $r = 300$. For large χ_s and r, layers $i \geq 2$ close to the surface are virtually empty of A segments. For example, at $\chi_s = 20$ and $r = 300$ the quantity $(r/r_A)\varphi_{Ai}$ remains below 10^{-5} in layers 2–10 and slowly rises to within 1% of its asymptotic value over layers 11–53.

Variation of Interfacial Tension. As the preferentially adsorbing A segments concentrate at the interface with increasing χ_s it is expected that the interfacial free energy of the system will decrease. In Figure 2 we present the variation of the nondimensionalized interfacial free energy

$$\epsilon = \frac{\gamma a}{kT} - \frac{u_s^B}{kT} \tag{2}$$

relative to a pure monomeric liquid, consisting of type B segments, as a function of the interaction parameter χ_s for various chain lengths. Computations were based on eq 68 of ref 1.

For $\chi_s = 0$, ϵ assumes a value ϵ_{B_r}, characteristic of a pure homopolymer of degree of polymerization r, consisting of type B segments. The dependence of ϵ_{B_r} on chain length r, as predicted by our site model, has been presented in ref 5, top part of Figure 2. The entire contents of that figure are collapsed at the origin of Figure 2 of the present paper. For values of $\chi_s > 0$ much more dramatic changes in interfacial tension and its dependence on chain length are observed. To obtain a quantitative feeling of how γ scales with r and χ_s we correlated our results, at each chain length studied, by a power law equation of the form

$$\epsilon(0,r) - \epsilon(\chi_s,r) = \epsilon_{B_r}(r) - \epsilon(\chi_s,r) = D_r\chi_s^{E_r} \tag{3}$$

Equation 3 was found to describe our model results quite accurately. Parameter values for various chain lengths, determined by nonlinear regression, using the Harwell subroutine VA10A,[6] are listed in Table II. The exponent E_r is seen to vary between 1.42 and 1.78 in the range of chain lengths examined. A global regression on all surface energy results was also tried; its performance was somewhat less satisfactory than that of the individual, constant-r regressions of Table II (root-mean-squared deviation between actual and regressed results 0.092). On the basis of this global regression, interfacial tension scales with χ_s and r according to the law

$$\epsilon(0,r) - \epsilon(\chi_s,r) = 0.31565\chi_s^{1.5258}r^{-0.5243} \tag{4}$$

The interfacial tension of bulk AB_{r-1} systems increases with increasing chain length, r, at fixed χ_s. This increase is expected from the fact that the mean concentration of the surface-loving A segments decreases in direct proportion to r^{-1}. The appearance of an r exponent closer to $-1/2$ than to -1 on the right-hand side of eq 4 reflects the fact that the interfacial system reorganizes itself, so as to expose the preferentially adsorbing A segments to the surface. This reorganization is also evident from the density profiles of Figure 1, discussed above.

Table II
Results from Fitting a Power Law Expression to the Dependence of Interfacial Tension on the Interaction Parameter χ_s[a]

$$\epsilon(0,r) - \epsilon(\chi_s,r) = \frac{(\gamma a)_{B_r} - (\gamma a)_{AB_{r-1}}}{kT} = D_r\chi_s^{E_r} \tag{3}$$

r	D_r	E_r	rms[b] dev betwn model results and eq 3
5	0.18007	1.4205	0.020
10	0.10368	1.4935	0.029
25	0.05193	1.5645	0.022
50	0.02995	1.6229	0.015
75	0.02113	1.6665	0.015
100	0.01762	1.6737	0.017
300	0.007158	1.7765	0.010

[a] Predicted by our lattice model in bulk AB_{r-1} systems. [b] Root-mean squared.

Bond Orientation Characteristics. Bond orientation in a pure homopolymer ($\chi_s = 0$), adsorbed on a solid surface, has been examined in ref 5. It was shown there that the presence of an interface causes bond orientation to depart from isotropy, characteristic of the unconstrained bulk. In the homopolymer case, orientation effects were found to be significant only within a narrow region, approximately six layers thick, for all chain lengths studied.

In the AB_{r-1} systems examined here the preferential adsorption of A segments on the surface is expected to cause significant deviations of bond orientation from isotropy in the interfacial region. All chains will strive to expose their adsorbing heads to the surface, as this reduces the Helmholtz energy of the system. A situation of congestion is thus expected, whereby conformations elongated in a direction perpendicular to the surface prevail, and bonds are preferentially directed perpendicular, rather than parallel, to the surface.

The numbers of bonds per surface site, n_{bi}^L and n_{bi}^T, emanating from each layer in directions perpendicular and parallel to the surface were calculated for all systems studied, by using eq 79, 82, and 83 of ref 1. Results, normalized by the corresponding unconstrained bulk limit values, one presented in Figures 3 and 4. For $\chi_s = 0$ (homopolymer case) it is seen that both quantities n_{b1}^L and n_{b1}^T exceed their unconstrained limit values. This is because of the impenetrability of the surface, as a result of which all bonds starting in layer 1 must either lie flat in layer 1 or connect layers 1 and 2. The quantities n_{bi}^L and n_{bi}^T decrease as we move from layer 1 to layer 2, where back stepping of bonds is no longer prevented by the surface. This decrease is observed in all cases studied, for both zero and positive values of the interaction parameter χ_s.

For a given chain length an increase in the value of χ_s is accompanied by an increase in the number of bonds

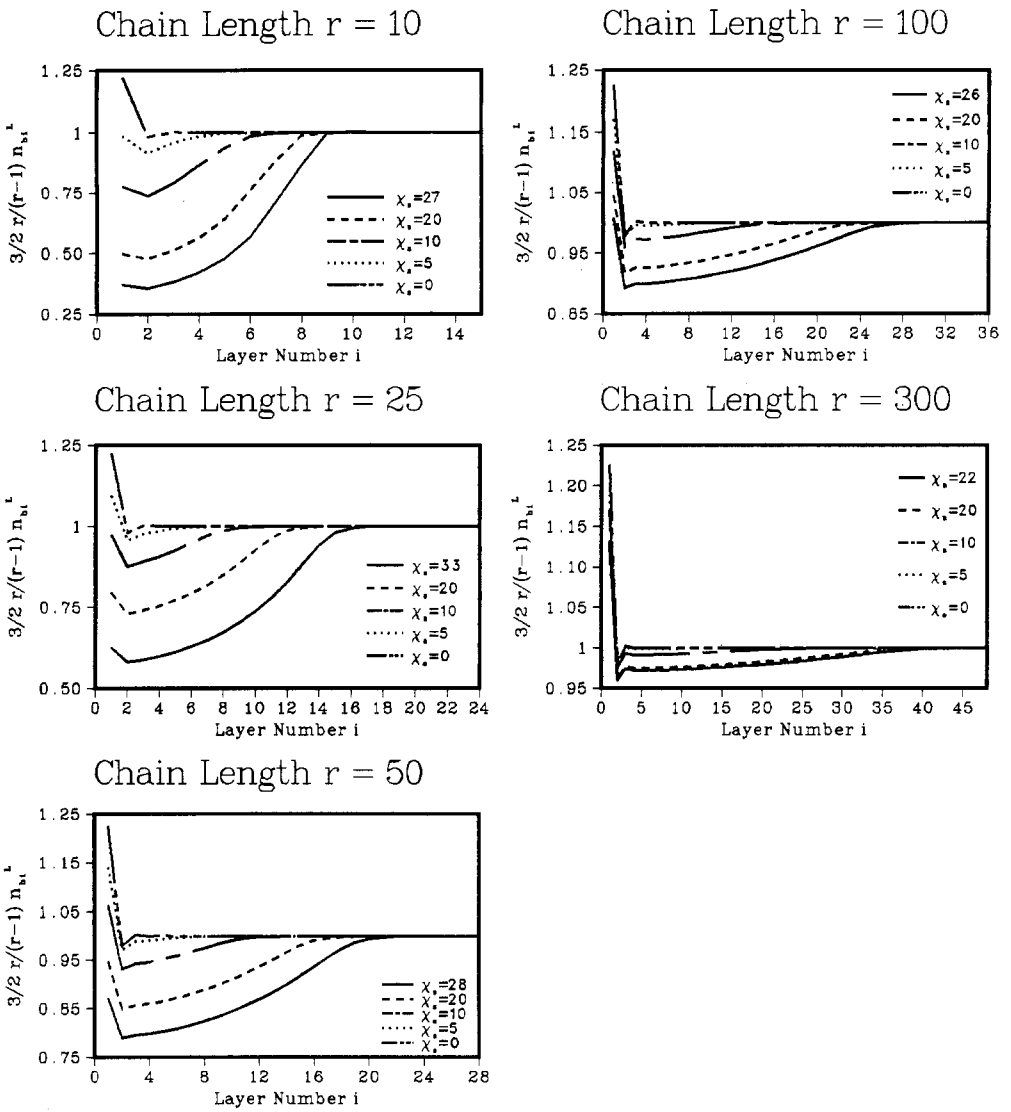

Figure 3. Number of bonds per surface site n_{bi}^{L} lying flat in layer i as a function of the layer number i in bulk AB_{r-1} systems, for various values of the interaction parameter χ_s. The quantity n_{bi}^{L} has been reduced by dividing with the asymptotic value $^2/_3(r-1)/r$, corresponding to the unconstrained bulk limit. Chain length: $r = 10$; $r = 25$; $r = 50$; $r = 100$; $r = 300$.

directed perpendicular to the surface, at the expense of bonds parallel to the surface; also, the interfacial layer thickness over which bond direction anisotropy is observed increases with increasing χ_s. These observations are in accordance with what is expected on the basis of the preferential adsorption of chain heads, as discussed above. At a given value of χ_s the tendency for perpendicular orientation of bonds with respect to the surface is greatest at short chain lengths. This is a consequence of the relative scarcity of A segments in the high molecular weight systems, as well as of the ease with which shorter chains can rearrange their conformation to accommodate specific interactions at the interface. The thickness of the interfacial region, over which deviations from isotropy are observed, increases with increasing chain length. A comparison of Figures 1 and 4 shows that, at large values of χ_s, bond direction anisotropy is detectable over the same region, in which the concentration of A segments deviates significantly from its unconstrained bulk value.

As seen in Figure 4, the perpendicular bond profile n_{bi}^{T} starts at high values and decreases to a shallow minimum, prior to assuming its asymptotic unconstrained bulk limit. The minimum is observed in all cases studied; it is most pronounced at high χ_s and low r. It is most probably caused by termination of elongated chains, adsorbed on the surface; as a result of this termination the perpendicular bond flux is interrupted. From the point of view of mechanical properties in the glassy state it implies the presence of a weak spot in the transverse elastic modulus,[2] at which cohesive failure of the interfacial system could occur.

To complete the picture of bond orientation in our interfacial model systems, we present bond order parameter profiles, computed according to eq 87 of ref 1, in Figure 5. This figure characterizes local orientation as a function of distance from the interface, as determined by the relative numbers of perpendicular and parallel bonds; its information content, however, is less than that of Figures 3 and 4 taken together, because it does not give us the total numbers of bonds in each layer. The profiles plotted in Figure 5 for $\chi_s = 0$ constitute a graphical representation of the pure homopolymer results reported in ref 5, Table III. Positive χ_s values lead to significant buildup of perpendicular orientation, the extent of the anisotropic region increasing with increasing molecular weight. The orientation effects induced by a given value of χ_s become weaker, as chains become longer and longer. The special conditions prevailing in the first layer, as well as the shallow minimum exhibited by S_i before it assumes its asymptotic unconstrained bulk limit of 0, have been discussed above. To quantitatively explore the spatial extent of bond orientation anisotropy we defined an interfacial

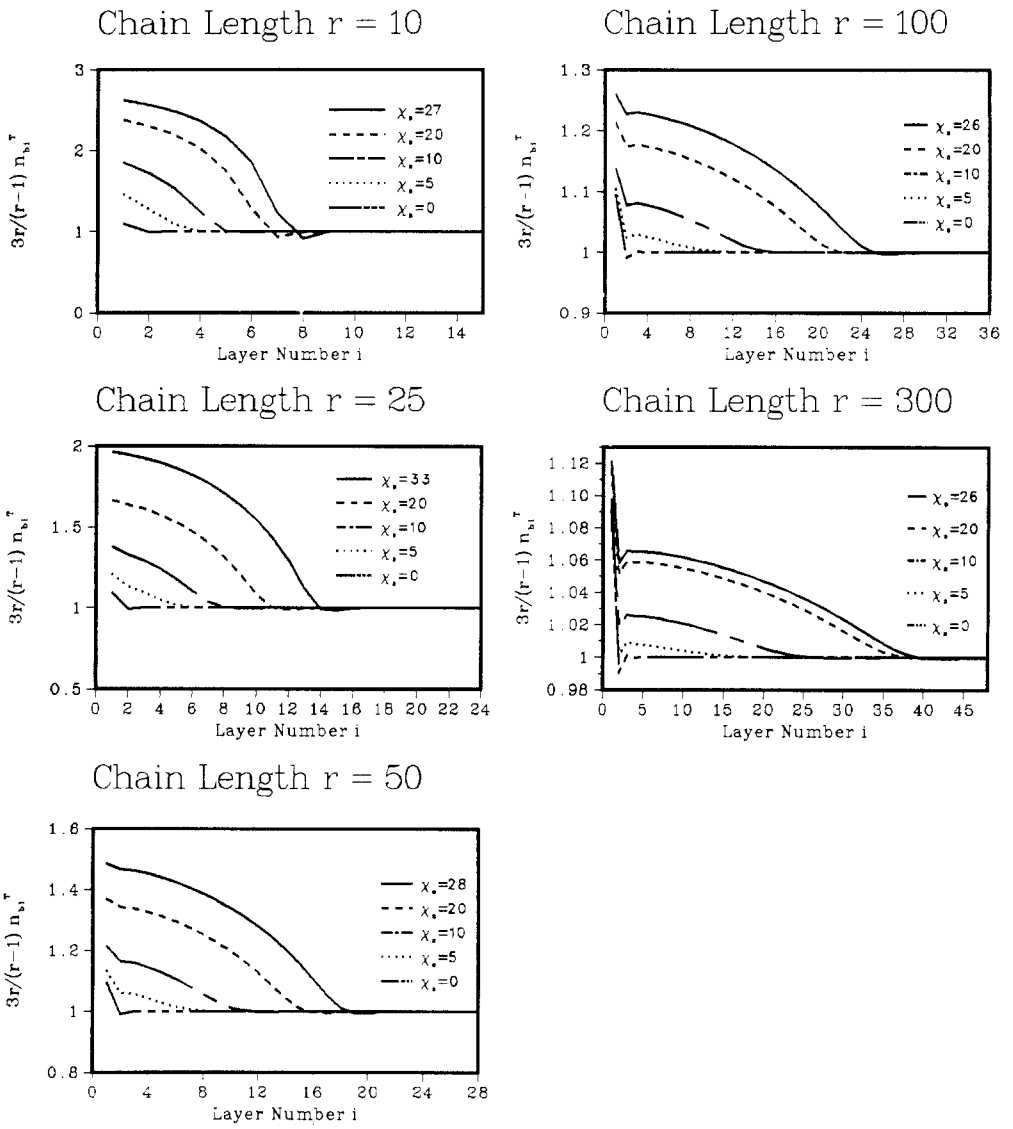

Figure 4. Number of bonds per surface site n_{bi}^{T} connecting layers i and $(i + 1)$ as a function of the layer number i in bulk AB_{r-1} systems, for various values of the interaction parameter χ_s. The quantity n_{bi}^{L} has been reduced by dividing with the asymptotic value $^1/_3(r - 1)/r$, corresponding to the unconstrained bulk limit. Chain length: $r = 10$; $r = 25$; $r = 50$; $r = 100$; $r = 300$.

thickness, h, as that value of i beyond which the absolute value of S_i never exceeds 10^{-5}:

$$h = i : |S_j| \leq 10^{-5}; \qquad \text{for all } j \geq i \tag{5}$$

The thickness h is a function of χ_s and r. We correlated our model results by the following double power law expression, using a reliable nonlinear regression algorithm:[6]

$$h(\chi_s,r) - h(0,r) = 0.31852\chi_s^{0.6255}r^{0.5124} \tag{6}$$

As mentioned above, $h(0,r) = 6$ for all values of r. Equation 6 describes our results quite satisfactorily (root-mean-squared deviation between actual and regressed values of h is 0.76). An interesting observation is that eq 4 and 6, taken together, imply that the product $\Delta h \Delta\epsilon$ is almost independent of chain length.

Chain Shape Characteristics. The number of chains per surface site, n_i, passing through layer i, and the average number of segments, n_{si}, that a chain passing through layer i occupies in that layer were calculated as functions of the layer number i, for all systems studied, by using eq 103 and 90 of ref 1. Results on n_{si}, which reflect perturbations in chain shape imposed by the presence of the interface, are reported in Figure 6. Values of n_{si} have been reduced by the asymptotic value $n_{s\infty}$, characteristic of the unconstrained bulk. As expected on the basis of model assumptions and the fact that $\chi = 0$, $n_{s\infty}$ is independent of copolymer chain composition and identical with the corresponding value for the pure homopolymer. Its dependence on chain length has been plotted in ref 5, Figure 3.

The reduced profiles of Figure 6 provide direct evidence of the elongation of individual chain conformations normal to the surface, as chains crowd themselves to expose their surface-active heads to it. In the pure homopolymer case, examined in ref 5, chains are clearly flattened parallel to the interface. This is a consequence of the purely entropic constraints imposed on the system by the solid wall. As chain heads become surface active ($\chi_s > 0$) there is a tendency for chains to crowd themselves near the surface, so as to take advantage of the energy benefit resulting from the adsorption of A segments. This lengthens chains in a direction perpendicular to the interface. As a result of the balance between entropic and energy effects, the profile $n_{si}/n_{s\infty}$ may exhibit a minimum or steadily increase from the first layer on, depending on the values of χ_s and r. For a given value of χ_s perturbations in chain shape move deeper into the polymer as chain length increases. A comparison of Figures 5 and 6 shows that such shape perturbations tend to persist somewhat deeper into the polymer than bond direction anisotropy effects induced by the surface. Contrary to what happens with bond orientation, which becomes more and more isotropic as

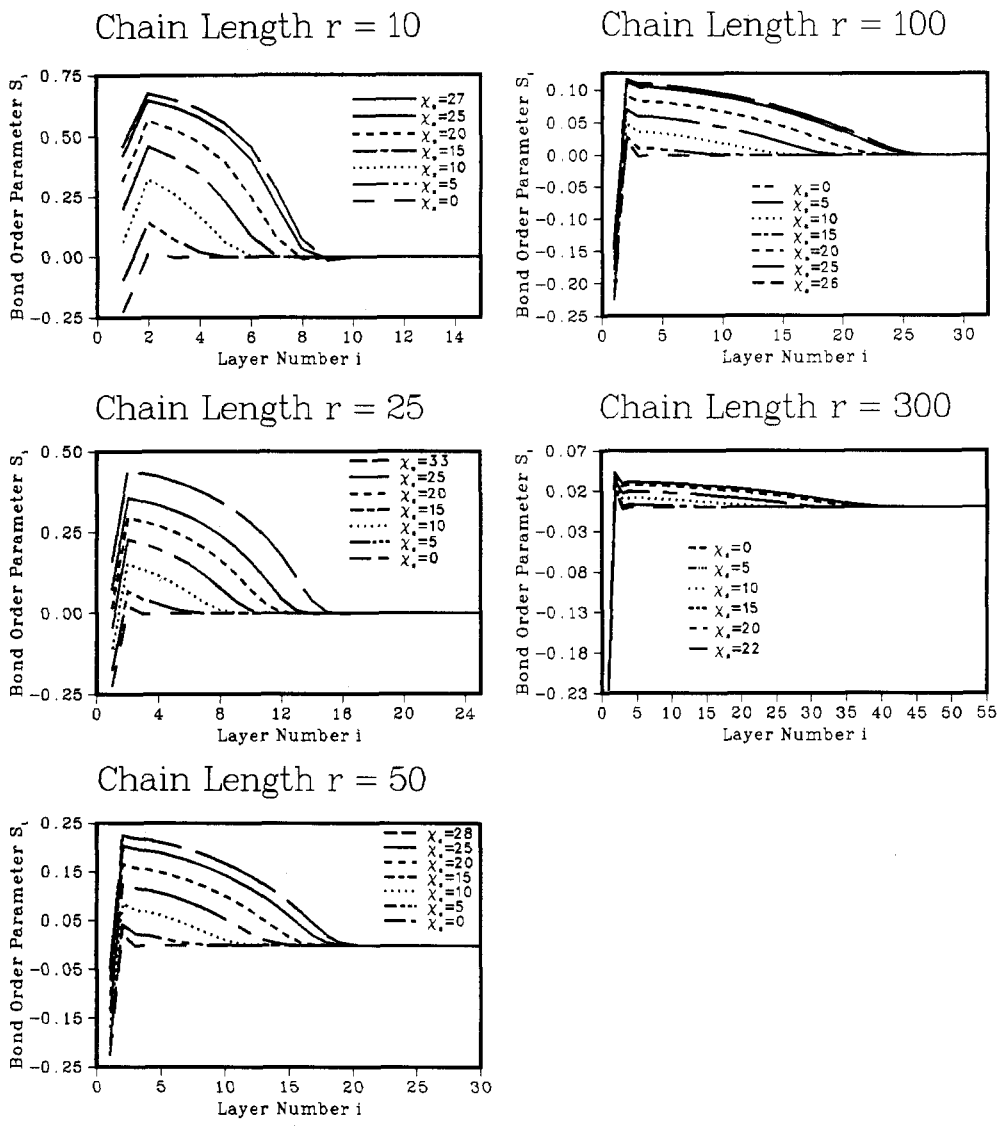

Figure 5. Bond order parameter profiles S_i in bulk AB_{r-1} systems, for various values of the surface interaction parameter χ_s. Perfect perpendicularity to the surface corresponds to $S_i = 1$, perfect parallelity to the surface to $S_i = -1/2$, and a completely random arrangement to $S_i = 0$. Chain length: $r = 10$; $r = 25$; $r = 50$; $r = 100$; $r = 300$.

chain length increases, the narrowing of chains remains practically unaffected at high molecular weight. Indeed, in the limit of high r the shape profiles of Figure 6 are remarkably similar, if one scales the i axis appropriately. The weak maximum through which $n_{si}/n_{s\infty}$ goes prior to assuming its asymptotic unconstrained bulk value (most readily observed in the shape profiles for $r = 10$) is probably associated with adsorbed chain termination, as discussed above.

Comparison of Various Measures of Interfacial Structure. In Figure 7 we present a comparison of three measures of interfacial structure, introduced above. These are the volume fraction φ_{A1} of surface-active chain heads in the first layer, the number n_1 of adsorbed chains per surface site, and the number of bonds per surface site, $n_{b1}{}^T$, connecting layers 1 and 2. In a hypothetical situation of full coverage of all surface sites by chain heads, and consequent perfect orientation of all chains perpendicular to the surface, all these quantities would concide at a value of 1.

Several observations can be made on the basis of Figure 7. First, full occupancy of the surface by chain heads is never achieved, even at the highest values of χ_s studied. Given the requirement of equilibrium with the unconstrained bulk polymer (ref 1, assumption V) it is not easy to perfectly orient the surface-active chains at the interface, no matter how large the affinity of chain heads may be for the surface (compare section 3). Second, the quantities φ_{A1} and n_1 quickly become indistinguishable with increasing χ_s; a value of χ_s = 8–10 suffices to make these quantities agree to three significant digits at all chain lengths examined. At low values of χ_s, $\varphi_{A1} < \eta_1$; there may be chains which are attached to the surface by segments other than the surface-active head. The equality of φ_{A1} and n_1 at high χ_s indicates that every adsorbed chain must necessarily have its surface-active head in the first layer. It generally has B-type segments adsorbed on the surface, too, whose number can be determined from Figure 6 and Figure 3 of ref 5. A third observation in Figure 7 is that the number of perpendicular bonds $n_{b1}{}^T$ is always larger than n_1 and φ_{A1}. In other words, not all perpendicular bonds starting from the first layer emanate from A-type segments; there are perpendicular bonds emanating from B-type segments; moreover, there are bonds that may emanate from either A or B segments and that lie flat in layer 1, as indicated by the difference between $n_{b1}{}^T$ and 1. The $n_{b1}{}^T(\chi_s)$ and $\varphi_{A1}(\chi_s)$ curves become asymptotically parallel for high values of the interaction parameter χ_s. From Figure 7 one sees again that the buildup of structural anisotropy at the surface is most pronounced in the case

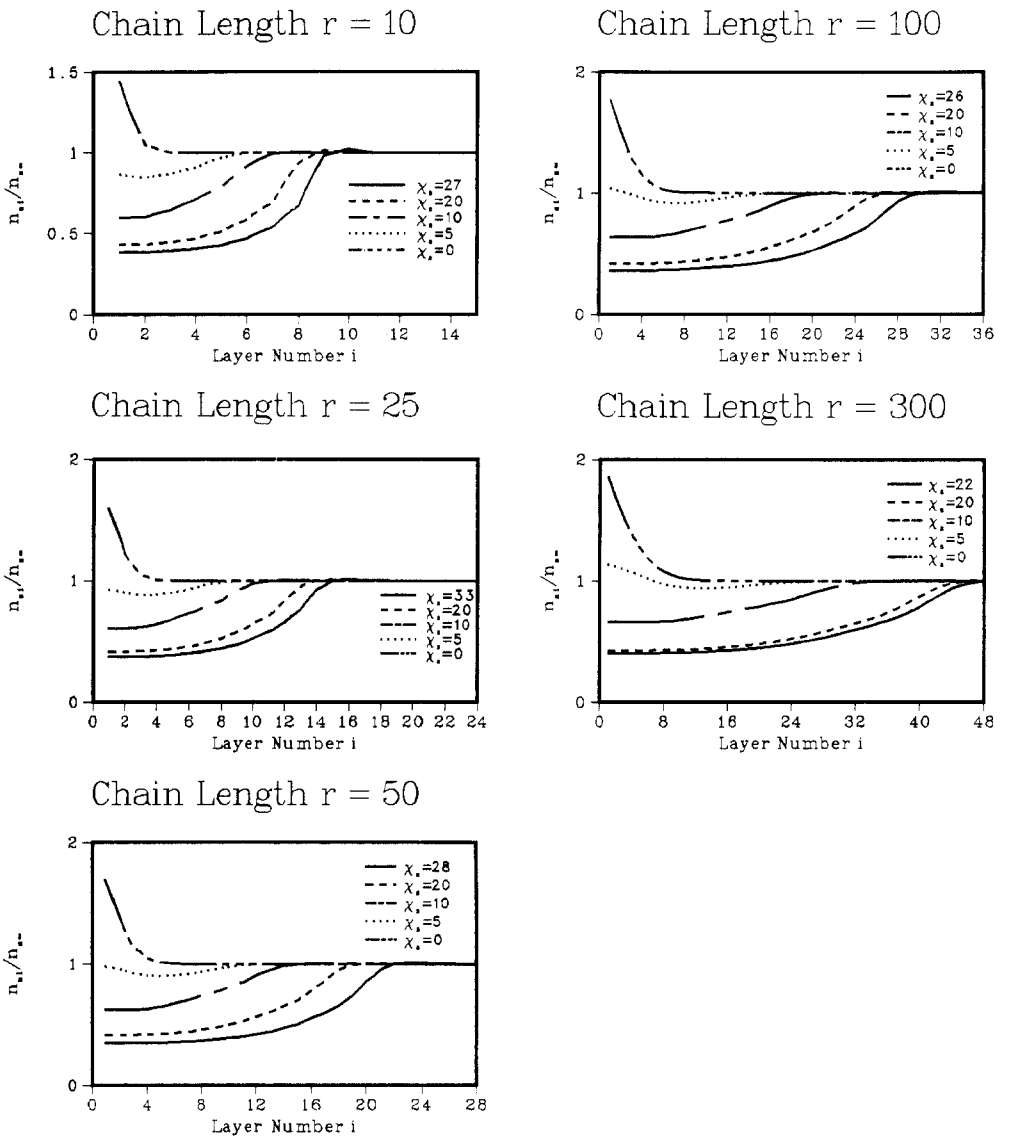

Figure 6. Reduced chain shape profiles in bulk AB_{r-1} systems, for various values of the interaction parameter χ_s. The quantity n_{si} is the average number of segments occupied by a chain passing through layer i in that layer; $n_{s\infty}$ is the asymptotic value assumed by n_{si} in the unconstrained bulk polymer. Chain length: r = 10; r = 25; r = 50; r = 100; r = 300.

of short chains. Also, among the quantities φ_{A1}, n_1, and $n_{b1}{}^T$, the latter (bond orientation) is the least sensitive to changes in the interaction parameter χ_s. For a system of chain length r = 300 it varies only little as χ_s sweeps the range 0–22.

The upper limits on χ_s listed in Table I for each chain length studied are close to the maximum values of χ_s for which convergence of the interfacial system of equations is achieved, using our zeroth-order continuation numerical scheme. Use of a finer step size $\Delta\chi_s$ made it possible to carry out the continuation to higher values of χ_s. Ultimately, however, divergence occurred, the Jacobian becoming singular in the vicinity of the expected solution. One might argue that values of χ_s as high as the upper limits listed in Table I are seldom realizable in physical systems. Nevertheless, the above-mentioned numerical behavior is indicative of the existence of a limit point with respect to the interaction parameter χ_s. Failure to converge beyond this point may signify that the interfacial system pictured by the model becomes unstable and must necessarily phase separate into an anisotropic adsorbed phase and an isotropic bulk phase, in equilibrium with each other. The virtual depletion of layers close to the surface of A segments, observed in Figure 1, and the appearance of structural features due to chain termination in Figures 4–6 suggest that such a phase separation at high χ_s values is plausible.

2. Surface Tension and Structure of Block and Random Copolymers

In this section we apply our interfacial lattice model to examine free surfaces of bulk liquid copolymers, consisting of two types of segments, A and B. Note that using a constant density, full occupancy model to represent melt/gas or melt/vacuum interfaces entails considerable abstraction and approximation. The segment density in such systems is expected to drop smoothly to zero as one passes from the liquid into the gaseous or vacuum phase; such a smooth variation is supported by recent Monte Carlo simulations of homopolymer melt surfaces.[7] We will assume that the length scale over which the density variation occurs is sufficiently short, so that we can approximate it by a sharp step and use our simple site model to explore the influence of chain architecture on interfacial structure and properties.

In view of the infinity of possible chain architectures that can be studied, we chose to confine ourselves to liquid copolymers whose surface tension has been measured experimentally. The systems examined here are closely modeled after the copolymers of ethylene oxide and pro-

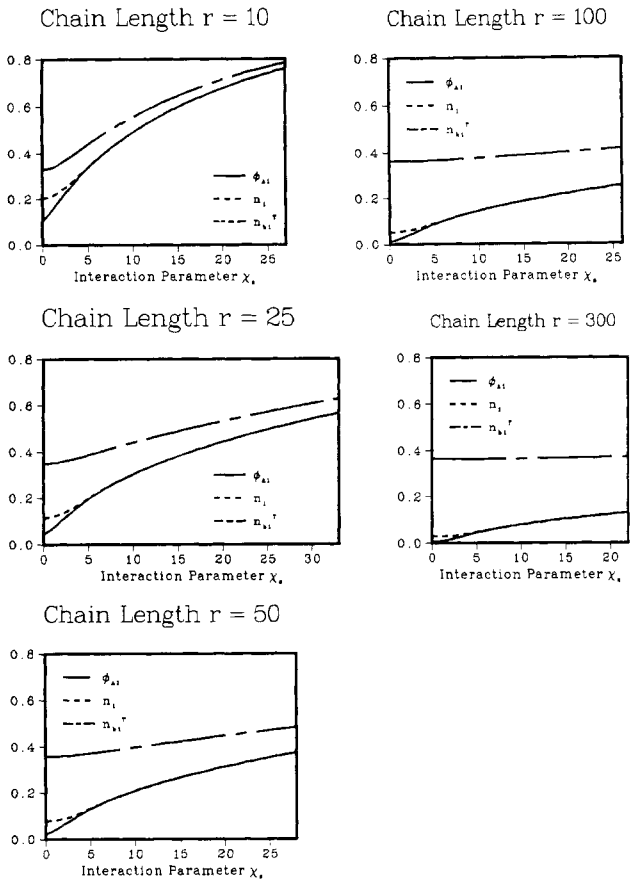

Figure 7. Comparison of three measures of interfacial structure in bulk AB_{r-1} systems; φ_{A1} is the volume fraction of A-type segments in the first layer, adjacent to the surface; n_1 is the number of adsorbed chains per surface site; $n_{b1}{}^T$ is the number of bonds per surface site emanating from the first layer in a direction perpendicular to the surface. Chain length: $r = 10$; $r = 25$; $r = 50$; $r = 100$; $r = 300$.

pylene oxide studied by Rastogi and St. Pierre.[8]

Our first task is to determine values for model parameters that represent the systems under examination. Relevant physical and thermodynamic properties are listed in Table III. We define the lattice site so that it can accommodate exactly one PEG unit. This is consistent with the common practice of taking a lattice segment as equivalent to three skeltal segments along the chain.[3] Then,

$$\text{lattice cell volume } V_{cell} = 38.9 \text{ cm}^3/\text{mol} = 64.59 \text{ Å}^3 \quad (7)$$

$$\text{lattice cell edge length } l = V_{cell}{}^{1/3} = 4.01 \text{ Å} \quad (8)$$

One PPG unit will then correspond to

$$\text{PPG unit} = 58.1/38.9 = 1.49 \text{ lattice segments} \quad (9)$$

The symbol B is used to designate the PEG (or high-surface tension) segments and the symbol A to designate the PPG (or low-surface tension) pseudo-segments, which will concentrate preferentially on the surface.

An estimate of the A–B segment interaction parameter χ is obtained from the solubility parameters as

$$\chi = \frac{V_{cell}}{RT}(\delta_{PEG} - \delta_{PPG})^2 = 0.004 \simeq 0 \quad (10)$$

which makes an analysis with $\chi = 0$ applicable.

To obtain the value of the interaction parameter χ_s, indicative of the tendency of A segments to adsorb on the surface preferentially over B segments, we use the pure homopolymer surface tension values reported by Rastogi

Table III
Physical and Thermodynamic Properties of Poly(ethylene oxide) (PEG) and Poly(propylene oxide) (PPG)

molar vol of units[a] (298 K, amorphous homopolymer bulk)		
PEG	$-CH_2CH_2O-$	38.9 cm³/mol
PPG	$-CH_2CH(CH_3)O-$	58.1 cm³/mol
surface tension[b] (298 K, pure homopolymer)		
PEG (degree of polymerization = 300)		43.5 dyn/cm
PPG (degree of polymerization = 2025)		31.2 dyn/cm
solubil param[c] (298 K, pure homopolymer)		
$\delta_{PEG} = 19.4$ J$^{1/2}$ cm$^{-3/2}$		
$\delta_{PPG} = 18.9$ J$^{1/2}$ cm$^{-3/2}$		

[a] Experimental values, ref 9, p 55. [b] Experimental values, reported in ref 8. Taken as representative of the infinite molecular weight polymers. [c] Most reliable values from cohesive energy, estimated by Van Krevelen–Hoftyzer method (ref 9, p 136) and experimental molar volume. Range of experimental solubility parameters reported for PPG: 15.4–20.3 J$^{1/2}$ cm$^{-3/2}$.

(Table III). Assuming these values to be representative of the infinite molecular weight polymer,

$$\gamma_{A\infty} = 31.2 \text{ dyn/cm} \qquad \gamma_{B\infty} = 43.5 \text{ dyn/cm} \quad (11)$$

Application of our model to a pure homopolymer has given[5]

$$\frac{\gamma_{A\infty}a - u_S{}^A}{kT} = \frac{\gamma_{B\infty}a - u_S{}^B}{kT} = 0.1841 \quad (12)$$

From eq 11 and 12,

$$\chi_s = -\frac{u_S{}^A - u_S{}^B}{kT} = \frac{\gamma_{A\infty}a - u_S{}^A}{kT} - \frac{\gamma_{B\infty}a - u_S{}^B}{kT} - \frac{(\gamma_{A\infty} - \gamma_{B\infty})a}{kT} = -\frac{(\gamma_{A\infty} - \gamma_{B\infty})l^2}{kT} = 0.48 \quad (13)$$

A model copolymer of composition $A_{r_A}B_{r_B}$ will represent a PPG/PEG copolymer of composition $(PO)_{0.669r_A}(EO)_{r_B}$. The mole fraction of propylene oxide units in the polymer will thus be

$$x_{PO} = \frac{0.669r_A}{0.669r_A + r_B} \quad (14)$$

and the weight fraction of propylene oxide units will be

$$w_{PO} = \frac{38.83r_A}{38.83r_A + 44r_B} \quad (15)$$

If $\epsilon = (\gamma a - u_S{}^B)/kT$ is the reduced surface energy calculated from the model, the surface tension will be found, according to eq 2, 8, 11, and 12, as

$$\gamma = \frac{kT}{a}\left(\frac{u_S{}^B}{kT} + \epsilon\right) = \gamma_{B\infty} + (\epsilon - 0.1841)\frac{kT}{l^2} = (38.80 + 25.55\epsilon)\frac{\text{dyn}}{\text{cm}} \quad (16)$$

Equations 10 and 13 establish values for interaction parameters. Equations 14 and 15 define the molecular representation to be used, in terms of the actual copolymer chain architecture. Equation 16 provides a link between model results and experimentally observable surface tension.

Block Copolymers. Rastogi and St. Pierre[8] present surface tension data at 298 K for a series of ethylene oxide–propylene oxide triblock copolymers of the type $(EO)_{r_B/2}(PO)_{16}(EO)_{r_B/2}$, with r_B equal to 4, 22, and 92. To

Table IV
Simulation of Triblock Copolymers of Ethylene Oxide and Propylene Oxide[a]

Model Results

chain struct	mole fractn A segms, r_A/r	mole fractn PO units x_{PO}	wt fractn PO units, w_{PO}	reduced surf energy, ϵ	predicted surf tension, γ, dyn/cm	fractional reduction in surf tension[b]
A_{24}	1.0	1.0	1.0	−0.3037	31.0	1.0
$BA_{24}B$	0.923	0.889	0.913	−0.2686	31.93	0.926
$B_2A_{24}B_2$	0.857	0.801	0.841	−0.2439	32.57	0.874
$B_6A_{24}B_6$	0.667	0.572	0.638	−0.1861	34.04	0.757
$B_{11}A_{24}B_{11}$	0.522	0.422	0.491	−0.1464	35.06	0.675
$B_{24}A_{24}B_{24}$	0.333	0.251	0.306	−0.08997	36.50	0.560
$B_{46}A_{24}B_{46}$	0.207	0.149	0.187	−0.04111	37.74	0.461
$B_{100}A_{24}B_{100}$	0.107	0.074	0.096	0.01496	39.18	0.346
$B_\infty A_{24}B_\infty$	0.0	0.0	0.0	0.1841	43.5	0.0

Experimental Data of Rastogi and St. Pierre (ref 8, Figure 5)

chain struct	wt fractn PO units, w_{PO}	measured surf tension, γ, dyn/cm	chain struct	wt fractn PO units, w_{PO}	measured surf tension, γ, dyn/cm
PPG	1.0	31.2	$(EO)_{46}(PO)_{16}(EO)_{46}$	0.186	36.1
$(EO)_2(PO)_{16}(EO)_2$	0.841	31.9	PEG	0.0	43.5
$(EO)_{11}(PO)_{16}(EO)_{11}$	0.489	33.7			

[a] B = one EO unit; A = 0.67 PO unit. [b] Defined as $(\gamma - \gamma_{B_\infty})/(\gamma_{A_{24}} - \gamma_{B_\infty})$.

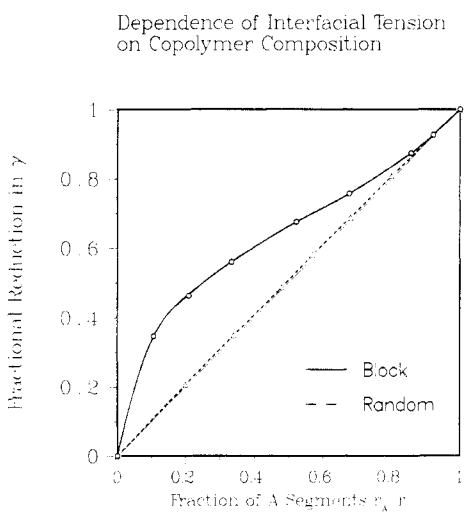

Figure 8. Dependence of interfacial tension on copolymer composition in triblock copolymers of the type $B_{r_B/2}A_{24}B_{r_B/2}$ and random copolymers of the type $A_{r_A}B_{100-r_A}$, according to our lattice model. The fractional reduction in interfacial tension relative to the pure B homopolymer is defined as $(\gamma - \gamma_{B_\infty})/(\gamma_{A_{24}} - \gamma_{B_\infty})$ in block copolymers and as $(\gamma - \gamma_{B_{100}})/(\gamma_{A_{100}} - \gamma_{B_{100}})$ in the random copolymer case.

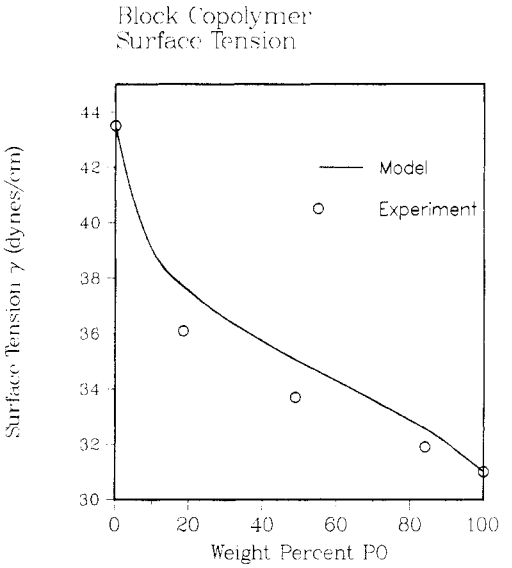

Figure 9. Variation of surface tension with weight percent PO in triblock copolymers of propylene oxide and ethylene oxide, of the general type $(EO)_{r_B/2}(PO)_{16}(EO)_{r_B/2}$. Continuous line, model predictions; points, experimental data of Rastogi and St. Pierre.[8]

simulate their measurements we applied our lattice approach to a series of model systems, having the structure $B_{r_B/2}A_{24}B_{r_B/2}$. Predicted surface tensions are shown in Table IV, together with experimental results, read off Figure 5 of ref 8.

At one end of the studied series of model block copolymer structures lies the pure homopolymer A_{24}; its surface tension can readily be obtained from γ_{A_∞}, as described in ref 5. At the other end lies the triblock copolymer $B_\infty A_{24}B_\infty$, whose interfacial behavior will be indistinguishable from that of pure B homopolymer of infinite molecular weight. We define the fractional reduction in surface tension relative to the pure B homopolymer, brought about by the introduction of A segments in the chain, as

$$\frac{\gamma - \gamma_{B_\infty}}{\gamma_{A_{24}} - \gamma_{B_\infty}}$$

where γ, $\gamma_{A_{24}}$, and γ_{B_∞} stand for the surface tensions of the triblock copolymer under examination, the pure homopolymer A_{24}, and the pure homopolymer B_∞.

In Figure 8 the fractional reduction in surface tension is plotted against the mole fraction of A segments in the chain (continuous line; numerical data listed in second and seventh columns of Table IV). The relationship between surface tension and composition is strikingly nonlinear. Introducing even a small block of A segments within the B chain results in a very significant reduction of surface tension. One can infer that copolymer chains rearrange themselves at the surface, so as to expose a maximum number of A segments to it, while at the same time avoiding the excessive decrease in entropy associated with highly ordered structures. The surface tension–composition curve follows a sigmoid shape and becomes asymptotically linear in the limit of pure A homopolymer.

A direct comparison of model predictions with Rastogi and St. Pierre's[8] surface tension data, listed in Table IV, is given in Figure 9, in the exact coordinates used by these authors in presenting their results. Experimental data

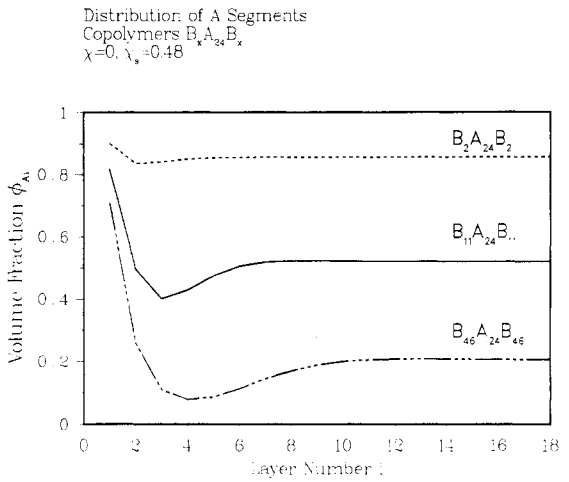

Figure 10. Spatial distribution of A segments in model systems of the type $B_xA_{24}B_x$, chosen to simulate triblock copolymers of ethylene oxide and propylene oxide.

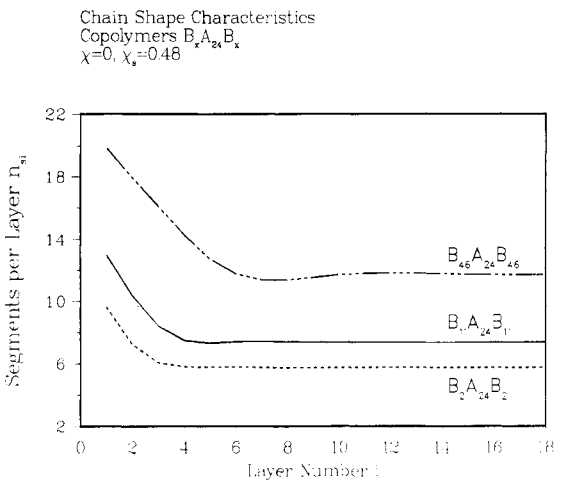

Figure 11. Chain shape profiles for model systems of the type $B_xA_{24}B_x$ chosen to simulate triblock copolymers of ethylene oxide and propylene oxide. The quantity n_{si} stands for the average number of segments that a chain passing through layer i has in that layer.

confirm the nonlinear dependence of γ on w_{PO}, predicted by the model. Predicted surface tensions tend to be higher than reported experimental values. This is probably a result of the sharp interface, constant density picture implicit in the lattice model, which limits the ability of chains to reorganize themselves in response to the special conditions prevailing at the interface. Nevertheless, in view of the fact that no adjustable parameters are involved and that there is considerable uncertainty as to the surface tension of the pure homopolymers used in Rastogi and St. Pierre's work, agreement between model and experiment is very satifactory.

Structural characteristics of our triblock copolymers in the vicinity of the surface, as predicted by the lattice model, are presented in Figures 10 and 11. The three structures examined in these figures correspond to the systems studied experimentally in ref 8 (compare Table IV).

A tendency for preferential exposure of A segments to the surface is clearly seen in Figure 10. This tendency is strongest in the case of the longest chain, $B_{46}A_{24}B_{46}$, in which the fraction of A segments is also lowest. Thus, the A-concentration profiles of Figure 10 explain the deviation from linearity toward low surface tension values, seen in Figures 8 and 9. In layers adjacent to the surface layer the volume fraction φ_{Ai} drops progressively to a minimum value and subsequently rises to its asymptotic, unconstrained bulk limit of r_A/r. The origin of this depletion phenomenon has been discussed in section 1: Layers close to layer 1 must necessarily accommodate the B segments belonging to the lateral blocks of chains whose middle block is preferentially adsorbed on the surface. Consistent with this interpretation, the location of the minimum in A volume fraction shifts to larger distances from the surface as the length of the lateral blocks increases. The overall width of the interfacial region, in which structural perturbations relative to the unconstrained bulk are detectable, does not exceed 13 lattice layers, or approximately 50 Å, in the case of the $B_{46}A_{24}B_{46}$ block copolymer. Note that A segment concentration profiles are much smoother for $B_{r_B/2}A_{r_A}B_{r_B/2}$ copolymers than they were for AB_{r-1} copolymers, examined in Figure 1. In other words, interfacial structure is more diffuse in the block copolymer case than in the case of a polymer with a single surface-active head.

The shape of our model block copolymer chains near the interface is examined in Figure 11. At large distances from the surface the number of chain segments per layer assumes an asymptotic value $n_{s\infty}$, characteristic of an unconstrained bulk homopolymer of the same chain length (compare ref 5, Figure 3). Near the surface, chains appear clearly flattened; the magnitude of this flattening effect is comparable to that observed in the pure homopolymer case (compare ref 5, Figure 4). The ratio $n_{s1}/n_{s\infty}$ is equal to 1.679, 1.790, and 1.679 for chains $B_2A_{24}B_2$, $B_{11}A_{24}B_{11}$, and $B_{46}A_{24}B_{46}$, respectively. The same ratio is equal to 1.615, 1.684, and 1.786 for the corresponding homopolymer chains B_{28}, B_{46}, and B_{116}, respectively. The high-molecular weight copolymer chains are actually less flat than homopolymer chains of the same chain length. This is because shape is primarily dictated by the preferentially adsorbing middle block. The competition of A-blocks for sites on the surface forces the B-tails out of the first layer and results in less flat conformations. An interesting feature of copolymer chain shapes, not present in the case of pure homopolymers, is the existence of a shallow minimum in the n_{si} profile. This minimum is most clearly seen in the $B_{46}A_{24}B_{46}$ curve of Figure 11. It exists in the case of $B_{11}A_{24}B_{11}$, as well. Its most probable cause is the termination of B side branches of chains adsorbed on the surface by their middle A blocks. As a significant proportion of chains passing through a layer i in the vicinity of the minimum participate in that layer only through the tapering ends of their dangling B-blocks, the average number of segments per chain n_{si} is lower than in the unconstrained polymer. Bond orientation effects, as probed by the quantities n_{bi}^L, n_{bi}^T, and S_i (not displayed here) in our block copolymer systems, are not very strong. There is a clear tendency for bonds to lie flat on the surface; this is more pronounced than the corresponding tendency in the bulk homopolymer and increases with increasing chain length. Ordering effects are quickly dissipated with increasing distance from the surface, however.

Random Copolymers. Rastogi and St. Pierre[8] present surface tension data for random copolymers of propylene oxide and ethylene oxide. The degree of polymerization of their samples is not reported. We assume here that it was on the order of 100. To simulate their data we generated Bernoullian sequences of A and B segments, of the general composition $A_{r_A}B_{r_B}$, where the relative proportion r_A/r_B was varied, but the total length $r_A + r_B = r$ was kept fixed and equal to 100. We applied our lattice model to bulk systems of chains whose architecture is defined by these sequences. The systems studied, and model predictions for the surface tension, are presented in Table V,

Table V
Simulation of Random Copolymers of Ethylene Oxide and Propylene Oxide[a]

Model Results

chain struct	mole fractn A segms, r_A/r	mole fractn PO units, x_{PO}	wt fractn PO units, w_{PO}	reduced surf energy, ϵ	predicted surf tension, γ, dyn/cm	fractional reduction in surf tension[b]
A_{100}	1.00	1.000	1.000	−0.2977	31.19	1.000
$A_{80}B_{20}$	0.80	0.729	0.779	−0.2056	33.54	0.808
$A_{68}B_{32}$	0.68	0.588	0.652	−0.1484	35.01	0.688
$A_{57}B_{43}$	0.57	0.471	0.539	−0.09650	36.33	0.581
$A_{48}B_{52}$	0.48	0.383	0.449	−0.05166	37.48	0.487
$A_{34}B_{66}$	0.34	0.257	0.313	−0.01477	39.17	0.349
$A_{20}B_{80}$	0.20	0.144	0.181	−0.08255	40.91	0.207
B_{100}	0.00	0.000	0.000	0.1823	43.45	0.000

Experimental Data of Rastogi and St. Pierre (Ref 8, Table III and Figure 1)

mol PO/ mol EO	mole fractn PO units, x_{PO}	measured surf tension, γ, dyn/cm	mol PO/ mol EO	mole fractn PO units, x_{PO}	measured surf tension, γ, dyn/cm
∞	1.000	31.2	0.61	0.379	37.8
1.44	0.590	34.2	0.35	0.259	39.2
0.87	0.465	36.3	0.00	0.000	43.5

[a] B = one EO unit; A = 0.67 PO unit. [b] Defined as $(\gamma - \gamma_{B_{100}})/(\gamma_{A_{100}} - \gamma_{B_{100}})$.

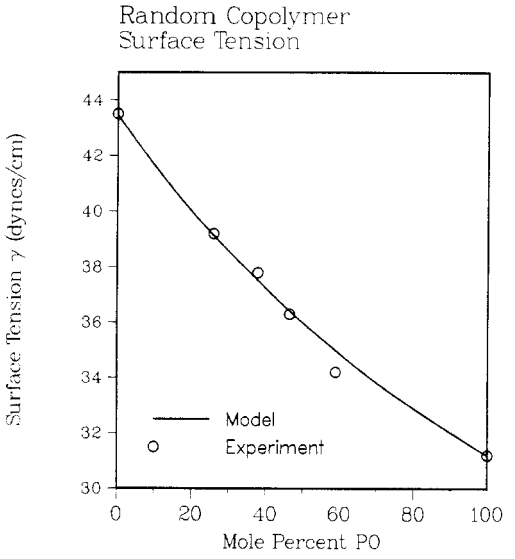

Figure 12. Variation of surface tension with mole percent PO in random copolymers of propylene oxide and ethylene oxide. Continuous line, model predictions; points, experimental data of Rastogi and St. Pierre.

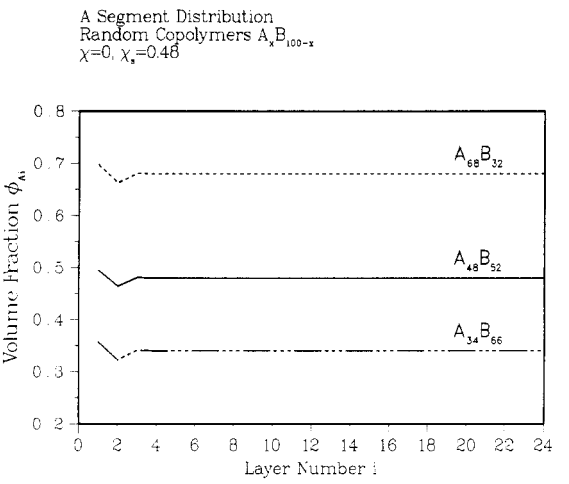

Figure 13. Spatial distribution of A segments in model systems of the type A_xB_{100-x}, chosen to simulate random copolymers of ethylene oxide and propylene oxide.

together with the corresponding experimental results from ref 8.

We define the fractional reduction in surface tension, brought about by the presence of A segments in the chain, as the ratio

$$\frac{\gamma - \gamma_{B_{100}}}{\gamma_{A_{100}} - \gamma_{B_{100}}}$$

where γ, $\gamma_{A_{100}}$, and $\gamma_{B_{100}}$ stand for a surface tension of a random copolymer of given composition, a pure A homopolymer, and a pure B homopolymer, all consisting of $r = 100$ segments. The fractional reduction in surface tension is plotted as a function of the mole fraction of A segments in the chain in Figure 8 (broken line; numerical data given in the second and seventh columns of Table V). The relationship is almost perfectly linear (there is actually a very slight deviation toward low γ values), in sharp contrast to what is observed in the block copolymer case. This is an immediate consequence of chain architecture. Since A segments are randomly distributed along the entire chain length, a chain cannot preferentially expose them to the surface, without also exposing the neighboring B segments.

Model predictions for the surface tension are compared directly to the experimental data of Rastogi and St. Pierre in Figure 12; again, the coordinates used in ref 8 have been selected. The agreement is excellent. In their publication Rastogi and St. Pierre state that γ is a linear function of x_{PO}. The straight line they present in Figure 1 of ref 8, however, when extrapolated to the limit $x_{PO} = 1$, gives an unreasonably low value for the surface tension of the pure PPG homopolymer. Our lattice model provides a consistent picture of the situation: γ is a practically linear function of r_A/r; when plotted against x_{PO}, however, it renders a curve which is concave downward, as a result of the difference in molar volume between PO and EO units.

The interfacial structure of three random copolymers, representative of the systems studied experimentally in ref 8, is explored in Figures 13 and 14. The volume fraction of A segments shows deviations from its asymptotic, unconstrained bulk value of r_A/r only in the three first lattice layers. Chain shape profiles coincide for all random copolymer chains examined; they are practically identical with that of a pure homopolymer of the same degree of polymerization. As noted above, the random

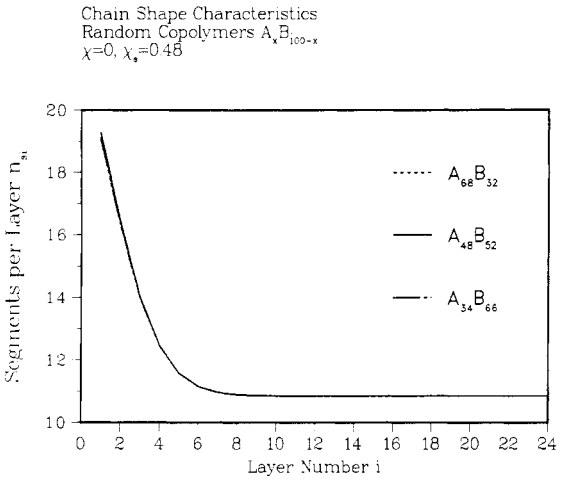

Figure 14. Chain shape profiles for model systems of the type A_xB_{100-x} chosen to simulate random copolymers of ethylene oxide and propylene oxide. See legend to Figure 11.

mixing of A and B segments along the copolymer chain does not allow it to reorganize its conformation, so as to take advantage of the specific interactions that exist between A segments and the surface. Bond order parameters (not shown here) were found to alternate between negative and positive values, in a manner very reminiscent of the pure homopolymer bulk (compare ref 5).

3. Chain Conformation in Lipid Bilayer Membranes

Short surface-active molecules, of the type studied in section 1, are representative of lipids and soaps, formed of a polar head and a hydrocarbon tail. Lipid/water systems exhibit interesting microphase separation phenomena, crucial to the understanding of biological membranes. In the lamellar (L_α) phase a periodical stacking of lipid and water lamellae is observed. A lipid lamella consists of a bilayer of surface-active molecules, with their polar heads adsorbed at the two lipid/water interfaces, and their hydrophobic tails propagating toward the interior of the lamella. The bilayer thickness is commensurate to twice the length of the lipid molecule, and is a decreasing function of temperature. For dipalmitoyl lecithin bilayers of 5% water content, for example, it ranges[10] from 48.3 Å at 35 °C to 36.7 Å at 39 °C. At low temperatures hydrocarbon chains in a lamella are thought to exhibit perfect crystalline order.[11] At higher temperatures a disorder gradient develops as a function of distance from the interface. Near the interface chains are closely packed and highly ordered. At the center of the bilayer a disordered situation, analogous to that in a liquid hydrocarbon, is thought to prevail. Chains are mobile and flexible, their average length being shorter than that of a fully extended chain, as evidenced by the decrease in bilayer thickness.

The structure of lipid bilayer membranes in the high-temperature L_α phase has been probed experimentally in considerable detail. In particular, NMR data from systems of selectively deuteriated lipids[10,11] provide direct evidence on the average orientation of various bonds along the lipid chains.

A simple lattice model for the description of bond orientation characteristics in lipid bilayers has been proposed by Dill and Flory.[3] The mathematical structure of this model has been examined in ref 2, where it was shown that it belongs to the general category of bond models and achieves closure by introducing the assumption

$$b_i^+ = 0 \qquad (17)$$

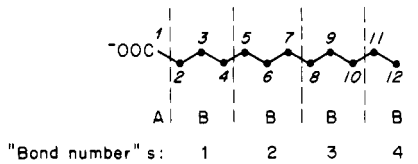

Figure 15. Assignment of the model structure AB_4 to potassium laurate, $CH_3(CH_2)_{10}COO^-K^+$.

for the (conditional) back-stepping probability of bonds in the positive direction (from hydrophilic head to hydrophobic tail) along the chain. In this section we apply our site lattice approach to a lipid bilayer, aiming at a comparison of its predictions on bond orientation with the corresponding predictions of the Dill and Flory model and with experimental evidence.

The physical situation on which we focus is a bilayer of potassium laurate in a $CH_3(CH_2)_{10}COOK/H_2O$ system, containing 24% H_2O, at a temperature of 50 °C. NMR data from this system have been presented in ref 11.

Consistent with the usual lattice model picture,[3] we represent the laurate anion by the five-segment model structure AB_4, where A stands for the polar head and each B segment but the last stands for a triad of skeletal methylenes. The exact assignment of segments and bonds of the model structure to the real molecule is explained in Figure 15. The direction of bonds 1, 2, 3, and 4 of the model structure will be representative of the orientational situation around carbons 3, 6, 9, and 12 of the laurate chain, counted from the carboxyl head.

In a lipid bilayer membrane the polar head of every chain necessarily resides on one of the two boundaries between the membrane and the surrounding water phase. There are no heads in the interior of the membrane. Such a situation could, in principle, be achieved in our bulk model systems, if the number of layers m to the middle between the interfaces is chosen so that $m \leq r$. Our model, however, incorporates the additional assumption that the interfacial system is in equilibrium with bulk liquid unconstrained polymer of the type AB_4 (ref 1, assumption V). This equilibrium requirement does not exist in a real bilayer; the membrane is not in contact with a bulk lipid phase. Equilibrium with the unconstrained bulk will lead to the presence of A segments within the model bilayer, and the analogy with real bilayers breaks down.

Nevertheless, if m is chosen large enough ($m \gg 5$, semiinfinite system of bulk AB_4 at a single interface), the conformation of chains adsorbed at the model interface can provide an accurate picture of actual lipid conformation in half the domain of a bilayer membrane. As seen in Figure 1, at the high surface coverage typical of bilayer membranes (see below), layers adjacent to the first are practically depleted of A segments and interfacial structure is dominated by *adsorbed* chains. Whether these chains are bounded by similar chains, adsorbed at another interface, or by an unconstrained bulk of AB_4 does not make a difference in their bond orientation characteristics.

Thus, we chose to model half a potassium laurate bilayer by the top lattice layers of a bulk AB_4 system with m = 20 and χ = 0. The value m = 20 makes the model system effectively semiinfinite. The value χ = 0 ensures that chain heads that may be encountered in the interior of the model system will be interpreted as tails of chains attached to the opposite side of the bilayer.

Experimentally, the structure of bilayers in the high-temperature L_α phase has been found to be determined almost exclusively by the surface coverage, i.e., the number of polar heads per unit area.[3,10,11] For the potassium laurate bilayer considered here[11] the surface area per polar head

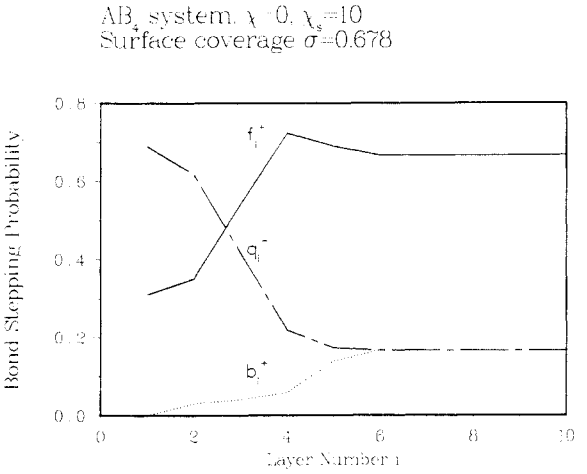

Figure 16. Forward-, side-, and back-stepping probabilities in the positive direction along the chain for a bulk AB_4 system, chosen to simulate a lipid bilayer of potassium laurate.

is 32.8 Å, which can be translated[3] into a fractional surface coverage of $\sigma = 0.62$. In our model surface coverage is a function of the interaction parameter χ_s. A value of $\chi_s = 10$ gives $\sigma = n_1 = \varphi_{A1} = 0.678$, close to the experimental coverage. The coincidence of n_1 and φ_{A1} at high χ_s has been discussed in section 1 (Figure 7). The value $\chi_s = 10$ was used in all bilayer modeling work reported here.

Contrary to the Dill and Flory model, our site model allows for back stepping of bonds toward the interface. Thus, it can be used to directly check the validity of the Dill and Flory assumption (17). Bond stepping probabilities f_i^+, q_i^+, and b_i^+ along the positive (head to tail) direction of chains, computed by using eq 72 of ref 1, are compared in Figure 16 for various layer numbers. As discussed above, the conformation of adsorbed chains predicted by the model in layers 1–5 is representative of half a potassium laurate bilayer. The back-stepping probability is indeed quite low in this region; it stays below 0.058 in the first four layers. The value of b_i^+ rises significantly in the fifth layer, but this does not affect adsorbed chains, which are the only relevant ones in the bilayer case (an adsorbed chain of four bonds cannot possibly back step on the fifth layer). Thus, even if complete flexibility is allowed, the Dill and Flory approximation of no back stepping is not unreasonable.

Most interesting is the bond disorder gradient existing in the bilayer. NMR measurements render an order parameter characteristic of the orientation of C–D bonds attached to specific skeletal carbons of deuteriated lipid molecules, with respect to the surface. From the C–D order parameters one obtains order parameters characteristic of skeletal bond orientation around each carbon atom in the lipid chain by simple multiplication by two.[10] It is the skeletal bond order parameter that we are concerned with here.

The question arises, with which model quantity should the experimental order parameter be compared. An order parameter S_i^+, characteristic of layer number i, can be formed from the bond stepping probabilities in that layer, by using eq 74 of ref 1. As pointed out above, however, experimental measurements give S not as a function of layer number or distance from the interface, but as a function of carbon number or bond number along the chain.

A quantity, which corresponds exactly to the experimentally measured order parameter, can be obtained from our model by averaging not over bonds lying in a given layer, but over bonds occupying a certain position along

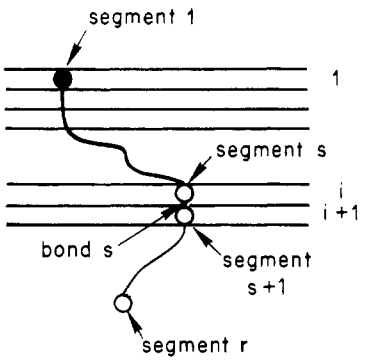

Figure 17. For the definition of the order parameter $S^+(s)$ as a function of bond number s in lipid bilayer systems.

an adsorbed chain, irrespectively of where exactly in the interfacial system these bonds are found. To define such a quantity we proceed as follows (Figure 17).

Consider an adsorbed chain. At the χ_s values of interest here the A-type head of the chain will necessarily lie in layer number 1. Consider the sth bond of the chain, counted from the polar head. This connects segments s and $s + 1$. Segment s may lie in any of the layers i, with $1 \le i \le s$. The subchain consisting of segments 1 to s is necessarily adsorbed. The probabilities that bond s propagates normal to the surface in the forward direction, parallel to the surface and normal to the surface in the backward direction, will be equal to

$$f^+(s) = \frac{\lambda_1 \sum_{i=1}^{2m} p^+_{(1)}(i,s)p^-(i+1,r-s)}{\sum_{i=1}^{2m} p^+_{(1)}(i,s)[\lambda_1 p^-(i+1,r-s) + \lambda_0 p^-(i,r-s) + \lambda_1 p^-(i-1,r-s)]} = \frac{\lambda_1 \sum_{i=1}^{u} p^+_{(1)}(i,s)p^-(i+1,r-s)}{\sum_{i=1}^{u} \frac{p^+_{(1)}(i,s)p^-(i,r-s+1)}{p_{t(s)i}}}$$

$$q^+(s) = \frac{\lambda_0 \sum_{i=1}^{2m} p^+_{(1)}(i,s)p^-(i,r-s)}{\sum_{i=1}^{2m} p^+_{(1)}(i,s)[\lambda_1 p^-(i+1,r-s) + \lambda_0 p^-(i,r-s) + \lambda_1 p^-(i-1,r-s)]} = \frac{\lambda_1 \sum_{i=1}^{u} p^+_{(1)}(i,s)p^-(i,r-s)}{\sum_{i=1}^{u} \frac{p^+_{(1)}(i,s)p^-(i,r-s+1)}{p_{t(s)i}}}$$

$$b^+(s) = \frac{\lambda_1 \sum_{i=1}^{2m} p^+_{(1)}(i,s)p^-(i-1,r-s)}{\sum_{i=1}^{2m} p^+_{(1)}(i,s)[\lambda_1 p^-(i+1,r-s) + \lambda_0 p^-(i,r-s) + \lambda_1 p^-(i-1,r-s)]} = \frac{\lambda_1 \sum_{i=1}^{u} p^+_{(1)}(i,s)p^-(i-1,r-s)}{\sum_{i=1}^{u} \frac{p^+_{(1)}(i,s)p^-(i,r-s+1)}{p_{t(s)i}}} \quad (18)$$

where $u = \min(2m,r)$ and the notation introduced in ref 1 has been used. From these probabilities an order pa-

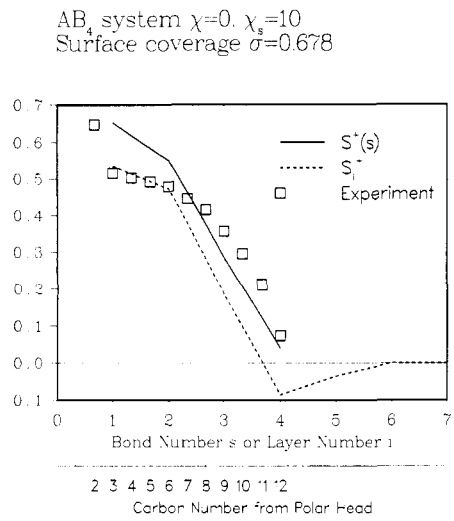

Figure 18. Skeletal bond-order parameters predicted by the model for a bulk AB_4 system, chosen to simulate a lipid bilayer of potassium laurate. Continuous line, order parameter $S^+(s)$ as a function of bond number s in adsorbed chains; broken line, order parameter S_i^+ as a function of layer number i from the surface; squares, experimental order parameters from NMR measurements.[11]

rameter $S^+(s)$, characteristic of the segment number s, is defined as

$$S^+(s) = \frac{1}{2}[3[f^+(s) + b^+(s)] - 1] = \frac{1}{2}[2 - 3q^+(s)] \qquad (19)$$

Model predictions on bond orientation in the bilayer are presented in Figure 18. The order parameter S_i^+, calculated from eq 74 of ref 1 for each layer number i, is plotted as a broken line; it corresponds to the order parameter reported by Dill and Flory.[3] The order parameter $S^+(s)$, calculated from eq 19 as a function of the bond number s, is plotted as a continuous line; as discussed above, it corresponds much more closely to the experimentally determined S. Order parameters from the NMR measurements of Mély, Charvolin, and Keller on potassium laurate membranes in mesophases with 24% by weight water content at 50 °C (ref 11, Figure 5) are also displayed in Figure 18.

Dill and Flory's calculation[3] was apparently based on a model system of only three lattice layers. Our S_i^+ profile is quite close to theirs, passing through the experimental points coresponding to carbons 3–6 and underpredicting order for carbons 2 and 7–12. As noted above, comparison S_i^+ to experimental data is not completely legitimate.

The $S^+(s)$ profile, which corresponds exactly to the experimental measurement, lies above the S_i^+ profile. It tends to overpredict order near the polar head, although the experimental point for carbon 2 indicates, beyond experimental error, that a degree of order as high as predicted by our $S^+(s)$ in fact exists in the immediate vicinity of the surface. The orientation predicted for the skeletal carbons 7–12 is close to experimental results. A point worth noting here is that S_i^+ and $S^+(s)$ profiles obtained from the Dill and Flory bond model practically coincide with each other in the case of a planar bilayer membrane.[3,12] Our site model, in contrast, indicates that a distinct difference between layer number based and bond order based order parameters should exist, as seen in Figure 18.

Agreement between our model predictions and experimental data on bond orientation in lipid bilayers must be considered quite satisfactory, especially in view of the several simplifications implicit in our representation of a bilayer. Notable among these simplifications are the use of effective segments and bonds to represent groups of segments and bonds of the real chain; the assumption of a lattice of constant density up to the bilayer surface, which does not allow for the possible presence of water molecules in the top layer, occupied by the polar heads; the use of a simple χ_s parameter to represent complex interactions, involving charged species at the interface; and the assumption of perfect flexibility, which does not take into account the intrinsic stiffness of the chains. Despite these assumptions, Figure 18, as well as Figures 9 and 12 of the previous section, indicates that the basic physical picture conveyed by the model is correct and useful in the quantitative description of a wide range of interfacial phenomena.

Conclusion

We have presented a lattice model for the quantitative prediction of structure (local composition, bond orientation, chain shape) and thermodynamic properties (surface tension, interfacial tension) of bulk polymers consisting of two types of segments at interfaces. A great variety of chain architectures can be studied with the model.

Only a few representative structures have been examined here. In bulk systems of surface-active polymers of the type AB_{r-1}, the preferential adsorption of A segments was found to lead to the development of perpendicular orientation of bonds with respect to the surface and to a narrowing of chain shapes within an interfacial region, whose thickness varies approximately with the square root of chain length; interfacial tension was explored quantitatively as a function of a parameter characterizing segment–surface interactions at the molecular level and as a function of chain length. In triblock copolymer systems of the type $B_{r_B/2}A_{r_A}B_{r_B/2}$ chains were found to reorganize themselves, so as to expose their preferentially adsorbing A segments to the surface; as a result, interfacial tension displays a nonlinear, convex dependence on chain composition. In random copolymer systems microscopic structure was predicted to be indistinguishable from that of a pure homopolymer, and a linear dependence of interfacial tension on chain composition was found. Model predictions for the surface tension of block and random copolymers of ethylene oxide and propylene oxide are in good agreement with experiment, without any adjustable parameters. Also, model predictions on bond orientation are consistent with NMR measurements on lipid bilayer membranes of potassium laurate.

These comparisons show that, despite the simplifying approximations built into the model, the basic physical picture is correct and useful in the quantitative exploration of structure–property relationships in a wide variety of relevant interfacial systems.

Results for systems characterized by a nonzero value of the interaction parameter χ have not been presented in this paper. Such systems can readily be examined, by using the model and the algorithmic approaches described in ref 1.

Future work will focus on the refinement of the assumptions that go into the model. First, the assumption of constant density throughout the interfacial region will be relaxed, by the introduction of voids in the lattice. We have developed a formulation for the description of the interfacial behavior of copolymer solutions, using the bidirectional approach we introduced in ref 1. Aside from its own merit for exploring solution systems of great technical importance, this formulation can readily be adapted to the bulk, with voids playing the role of solvent molecules. The inclusion of electrostatic forces, to represent ionic surfactant systems at aqueous interfaces, it

another interesting possibility; some ideas along these lines are presented by Koopal and Ralston.[13] Results from the above refinements and extensions will be reported in future publications.

Acknowledgment. Financial support was provided in the course of this work by the Director, Office of Basic Energy Sciences, Materials Science Division of the U.S. Department of Energy under Contact No. DE-AC03-76SF00098. Computing resources offered by Academic Computing Services at Berkeley are deeply appreciated. Support from the Shell Companies Foundation, in the form of a Faculty Career Initiation Fund, is gratefully acknowledged. We thank Dr. William Madden for making his manuscript available to us prior to publication.

List of Symbols

a area per surface lattice site
b_i bond back stepping probability in layer i
c conformation number
D_r constant appearing in power law fit of the dependence of the reduced interfacial tension ϵ on the interaction parameter χ_s, for a given value of the chain length, r (eq 3)
E_r constant appearing in power law fit of the dependence of the reduced interfacial tension ϵ on the interaction parameter χ_s, for a given value of the chain length, r (eq 3)
f_i bond forward stepping probability in layer i
h thickness of the anisotropic region of the interfacial system, defined by eq 5 (measured in lattice layers)
i layer number
k Boltzmann constant
l lattice edge length
L number of sites per layer
m half of the number of layers M
M number of layers of model interfacial system
n number of chains
n_{bi} number of bonds per surface site in layer i
n_c number of chains belonging to conformation c
n_i number of chains per surface site passing through layer i
n_{si} average number of segments per surface site that a chain passing through layer i has in that layer
$p^+(i,s)$ reduced end segment probability for an s-segment long subchain in layer i, in the positive direction
$p^-(i,s)$ reduced end segment probability for an s-segment long subchain in layer i, in the negative direction
p_{Ii} free segment probability of species I in layer i
q_i bond side stepping probability in layer i
r number of segments per chain
r_I number of I-type segments per chain (I = A, B)
s index for segments and bonds along a chain
S_i bond order parameter in layer i
$t(s)$ type of sth segment along the chain (may assume the values A, B)
T temperature
u_S^I adsorption energy of a segment of type I
V_{cell} lattice cell volume
w_{PO} weight fraction PO in EO/PO copolymer
x_{PO} mole fraction PO in EO/PO copolymer

Greek Symbols

γ surface tension; interfacial tension
δ solubility parameter
ϵ dimensionless interfacial free energy relative to a pure monomeric fluid of B segments, defined by eq 2
λ_0 fraction of nearest-neighbor sites to a given site lying in same layer as the considered site
λ_1 fraction of nearest-neighbor sites to a given site lying in the layer above (i.e., nearer the surface) the layer of the considered site; also, fraction of nearest-neighbor sites to a given site lying in the layer below the layer of the considered site
σ number of adsorbed chains per surface site in a model lipid bilayer membrane system; coincides with φ_{A1} and n_1
φ_{Ii} volume fraction of I-type segments in layer i (I = A, B)
χ Flory interaction parameter expressing the difference in interaction energy between unlike and like pairs of segments
χ_s surface interaction parameter, expressing the difference in affinities of the two types of segments for the surface

Superscripts

A pertaining to A-type segments
B pertaining to B-type segments
L longitudinal (in direction parallel to the surface)
T transverse (in direction perpendicular to the surface)
+ positive direction along the chain (head to tail)
− negative direction along the chain (tail to head)
* unconstrained bulk polymer

Subscripts

A A-type segment
A_r corresponding to pure A homopolymer of r units
b bond
B B-type segment
B_r corresponding to pure B homopolymer of r units
i pertaining to layer i
(i) chain passing through layer i
s segment; surface
∞ unconstrained bulk polymer, in the absence of interfaces

Registry No. (EO)(PO) (block copolymer), 106392-12-5; (EO)(PO) (copolymer), 9003-11-6; $H_3C(CH_2)_{10}CO_2K$, 10124-65-9.

References and Notes

(1) Theodorou, D. N. *Macromolecules*, preceding paper in this issue.
(2) Theodorou, D. N. *Macromolecules*, first of four papers in this issue.
(3) Dill, K. A.; Flory, P. J. *Proc. Natl. Acad. Sci. U.S.A.* **1980**, *77*, 3115–3119.
(4) Fowkes, F. M.; McCarthy, D. C.; Tischler, D. O. In *Molecular Characterization of Composite Interfaces*; Ishida, H., Kumar, G., Eds.; Plenum: New York, 1985; pp 401–411.
(5) Theodorou, D. N. *Macromolecules*, second of four papers in this issue.
(6) Fletcher, R. *U. K. At. Energy Res. Establ.*, [*Rep.*], *AERE-R* **1972**, *AERE-R7125*; subroutine VA10A in Harwell subroutine library, 1972.
(7) Madden, W. G. *J. Chem. Phys.* **1987**, *87*, 1405–1422.
(8) Rastogi, A. K.; St. Pierre, L. E. *J. Colloid Interface Sci.* **1969**, *31*, 168–175.
(9) Van Krevelen, D. W. *Properties of Polymers—Their Estimation and Correlation with Chemical Structure*, 2nd ed.; Elsevier: New York, 1976.
(10) Seelig, A.; Seelig, J. *Biochemistry* **1974**, *13*, 4839–4845.
(11) Mély, B.; Charvolin, J.; Keller, P. *Chem. Phys. Lipids* **1975**, *15*, 161–173.
(12) Dill, K. A.; Flory, P. J. *Proc. Natl. Acad. Sci. U.S.A.* **1981**, *78*, 676–680.
(13) Koopal, L. K.; Ralston, J. *J. Colloid Interface Sci.* **1986**, *112*, 362–379.